J. Med. Chem. **1998,** *41,* 778−786

Articles

High-Affinity Aptamers Selectively Inhibit Human Nonpancreatic Secretory Phospholipase A_2 (hnps-PLA_2)

Philippe Bridonneau,[†] Ying-Fon Chang,[†] Dan O'Connell,[†] Stanley C. Gill,[†] David W. Snyder,[‡] Lea Johnson,[‡] Theodore Goodson, Jr.,[‡] David K. Herron,[‡] and David H. Parma*[,†]

NeXstar Pharmaceuticals, Inc., 2860 Wilderness Place, Boulder, Colorado 80301, and Lilly Research Laboratories, Eli Lilly & Company, Indianapolis, Indiana 46285

Received August 29, 1997

A family of sequence-related 2′-aminopyrimidine, 2′-hydroxylpurine aptamers, developed by oligonucleotide-based combinatorial chemistry, SELEX (*s*ystematic *e*volution of *l*igand by *ex*ponential enrichment) technology, binds human nonpancreatic secretory phospholipase A_2 (hnps-PLA_2) with nanomolar affinities and inhibits enzymatic activity. Aptamer **15**, derived from the family, binds hnps-PLA_2 with a K_d equal to 1.7 ± 0.2 nM and, in a standard chromogenic assay of enzymatic activity, inhibits hnps-PLA_2 with an IC_{50} of 4 nM, at a mole fraction of substrate concentration of 4×10^{-6} and a calculated K_i of 0.14 nM. Aptamer **15** is selective for hnps-PLA_2, having a 25- and 2500-fold lower affinity, respectively, for the unrelated proteins human neutrophil elastase and human IgG. Contractions of guinea pig lung pleural strips induced by hnps-PLA_2 are abolished by 0.3 μM aptamer **15**, whereas contractions induced by arachidonic acid are not altered. The structure that is essential for binding and inhibition appears to be a 40-base hairpin/loop motif with an asymmetrical internal loop. The affinity and activity of the aptamers demonstrate the ability of the SELEX process to isolate antagonists of nonnucleic-acid-binding proteins from vast oligonucleotide combinatorial libraries.

Introduction

Human nonpancreatic secretory phospholipase A_2 (hnps-PLA_2) is a small (MW 13.9 kDa), secreted, cationic (p*I* 10.4), Ca^{2+}-dependent enzyme that catalyzes the hydrolysis of phospholipids at the *sn*-2 position.[1] Dramatically elevated levels of circulating hnps-PLA_2 are associated with numerous disease states, such as acute pancreatitis, adult respiratory distress syndrome (ARDS), bacterial peritonitis, and septic shock.[2] Yet, despite extensive studies, it has not been determined whether elevated hnps-PLA_2 levels are causal or merely symptomatic of disease.[3] Although it is plausibly and widely assumed that hnps-PLA_2-mediated toxicity is due to the enzyme's activity in producing arachidonic acid, the precursor of inflammatory eicosanoids, this assumption has not been verified. An interesting alternative, that hnps-PLA_2 facilitates complement fixation through a role in creating C-reactive protein binding sites on the membrane of damaged cells, has been proposed recently.[4] Two factors that have hindered efforts to define the role of hnps-PLA_2 are the existence of multiple enzymes with phospholipase A_2 activity and the lack of specific, high-affinity antagonists. Such antagonists are deemed essential for deciphering the biological role(s) of hnps-PLA_2.[5]

Rational drug design, one approach to developing improved antagonists, has produced an indole-based hnps-PLA_2 inhibitor, LY311727, which is superior to previously described antagonists in affinity, specificity, and inhibitory activity.[6] We have taken a very different approach, oligonucleotide-based combinatorial chemistry or SELEX (*s*ystematic *e*volution of *l*igand by *ex*ponential enrichment) technology,[7] to develop a hnps-PLA_2 inhibitor. SELEX technology utilizes iterative cycles of selection and amplification to isolate high-affinity aptamers to a specific target molecule from vast populations of sequence-randomized oligonucleotides. In this report, we describe the successful isolation of a family of sequence-related aptamers from a sequence-randomized, 2′-NH_2-pyrimidine, 2′-OH-purine RNA library. Aptamer **15**, derived from this family, is equivalent to LY311727 in affinity, specificity, and inhibitory activity.

SELEX

The rationale on which the SELEX process is based is that oligonucleotides have sequence-dependent secondary and tertiary structure. In a large population of sequence-randomized oligonucleotides, some have a tertiary structure that is complementary to the shape of the target molecule and consequently bind with high affinity. These high-affinity ligands can be isolated by cycles of selection and amplification. RNA, modified RNA, and single-stranded DNA (ssDNA) are suitable substrates for the SELEX process.

The SELEX process is initiated with a population of synthetic ssDNA molecules that contain a region of randomized sequence flanked by fixed sequences. The fixed sequences serve as primer annealing sites and, in RNA SELEX, contain a T7 RNA polymerase promoter

[†] NeXstar Pharmaceuticals, Inc.
[‡] Eli Lilly & Co.

S0022-2623(97)00579-7 CCC: $15.00
Published on Web 02/12/1998

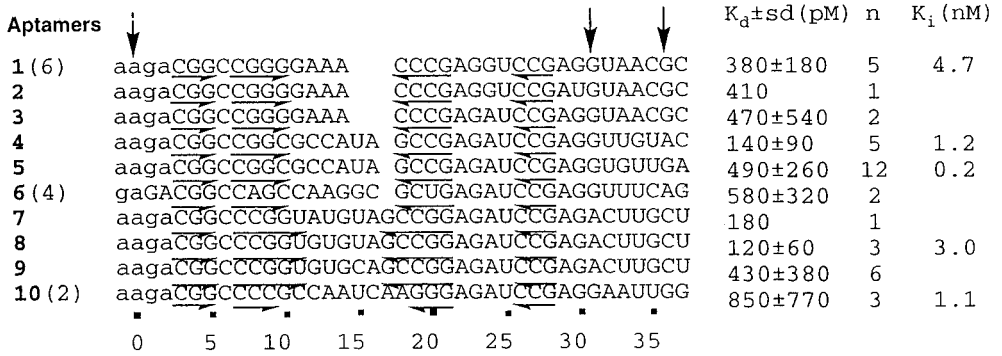

Figure 1. Family 1 aptamers: sequence alignment, affinities (K_d), and inhibition constants (K_i). Column 1 contains each aptamer's designation and, in parentheses, the number of times the sequence was isolated. The consensus portion of the variable region (upper case) and four nucleotides of the 5′-fixed region (lower case) are shown in column 2. Nucleotides at positions 8:20, 9:19, and 10:18 covary in Watson−Crick fashion. Opposing horizontal arrows indicate base-paired sequences (also see Figure 2). K_d, the mean and standard error of N independent, affinity determinations (see methods). The K_d listed for aptamer **2** is that of its high-affinity species. K_i, inhibition constant of hnps-PLA$_2$ enzymatic activity in TBK, pH 7.5, 10 mM $CaCl_2$, 10 mM hnps-PLA$_2$ (see methods). Vertical arrows indicate the positions of aptamer **5** boundaries (see Figure 4): 5′ boundary, position 0; low-stringency 3′ boundary, position 31; high-stringency 3′ boundary, position 36. Aptamers **1**, **6**, and **9**: 5′ boundaries, position 0; high-stringency 3′ boundaries, positions 38, 36, and 38, respectively (data not shown).

sequence. Synthetic ssDNA is converted to double-stranded (ds) molecules and amplified by polymerase chain reaction (PCR). For RNA SELEX, the dsDNA is then transcribed with T7 RNA polymerase. Purified transcripts are mixed with the target protein, and after suitable incubation, oligonucleotide/protein complexes are separated from unbound oligonucleotides. Commonly used partitioning techniques include filtration through nitrocellulose membranes, chromatography, immunoprecipitation, and gel electrophoresis. The bound oligonucleotides are then extracted from the RNA/protein complexes, reverse-transcribed, converted to dsDNA, amplified, and transcribed. These transcripts are the input pool for a new round of the SELEX process.

Starting pools contain as many as $10^{14}-10^{15}$ unique sequences. Each round enriches for sequences that bind with high affinity and reduces the pool's sequence complexity. Stringency of selection is increased by reducing the target protein's concentration, while maintaining oligonucleotide in excess. After several (usually 10−15) rounds or iterations of selection and amplification, when the affinity of the pool attains the desired value, dsDNA molecules derived from the selected aptamers are cloned, sequenced, and characterized.

Results and Discussion

Two alternative techniques were used to partition unbound RNA from hnps-PLA$_2$/RNA complexes during the SELEX process: (1) nitrocellulose filtration and (2) immobilization of hnps-PLA$_2$ on immunoaffinity beads. Standard SELEX protocols select aptamers for affinity exclusively, not for inhibition of target function. On the basis of observations that the active site of hnps-PLA$_2$ contains a bound calcium ion and that the binding of many evolved aptamers to hnps-PLA$_2$ is calcium-dependent,[8] we reasoned that elution in the absence of Ca^{2+} ions might facilitate the recovery of antagonists. To implement this strategy, we developed a new protocol in which hnps-PLA$_2$ was immobilized on immunoaffinity beads; bound ligands and/or hnps-PLA$_2$/RNA complexes were eluted by competition with polyclonal antibody in the absence of divalent cations. Subsequently, we have applied variations of this competitive and/or directed elution protocol to the isolation of aptameric antagonists of wheat germ agglutinin,[9] human L-selectin,[10,11] and both human and murine P-selectin.[12]

The starting pool for hnps-PLA$_2$ SELEX contained approximately 3×10^{14} RNA molecules (500 pmol) and bound hnps-PLA$_2$ with a K_d of 38 nM. After 11 rounds, the pool bound hnps-PLA$_2$ biphasically. The high-affinity species, two-thirds of the pool, bound with a K_d of 1.3 nM, a 29-fold improvement over the starting pool, while the low-affinity species, K_d of 48 nM, showed no improvement.

PCR products from the eleventh round were cloned and sequenced. Thirty-eight cloned ligands yielded 12 unique sequences or lineages. Nineteen ligands formed a family of related sequences (Figure 1). None of the remaining lineages displayed common sequence motifs. Aptamers of family 1 share two highly conserved sequences, CGGCCSGS,[13] adjacent to the 5′-fixed region, and WCWGAGRUCCGAGRY (Figure 1). Spacing between the two sequences varies from 4 to 9 nucleotides. Watson−Crick base-pairing patterns reveal that all family 1 aptamers contain a hairpin motif with an asymmetrical internal loop (Figure 2). The rules of comparative sequence analysis[14] suggest that the lower stem, the unpaired nucleotides adjacent to its base, and the asymmetrical internal loop, the family's most conserved sequences, are most apt to be directly involved in binding (Figures 1 and 2). The upper stem and terminal loop which vary in both sequence and length are less apt to be directly involved in binding. Three nucleotide pairs in the upper stem (8:20, 9:19, and 10:18, Figures 1 and 2) are supported by Watson−Crick covariation.

The affinities of representative family 1 aptamers for hnps-PLA$_2$, determined by nitrocellulose filtration, range from 120 to 850 pM (Figure 1). Aptamer binding is monophasic. An exception, aptamer **2,** binds in a biphasic manner. All family 1 aptamers bind with high affinity, while the affinities of non-family 1 aptamers (data not shown) are not significantly different from that of random RNA which suggests that the eleventh round pool contained a single, major high-affinity family and

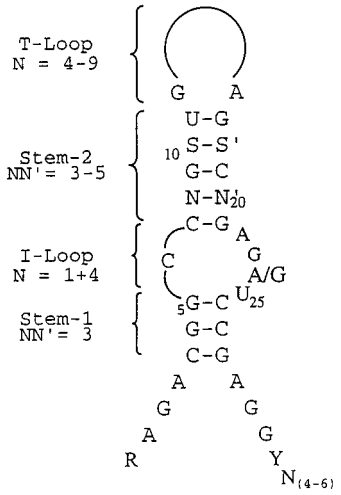

Figure 2. Deduced secondary structure of family 1 aptamers. The deduced structure is a hairpin with a sequence-conserved asymmetrical internal loop. Pairing of positions 8:20, 9:19, and 10:18 is supported by Watson−Crick covariation. Nucleotide sequence is in standard one-letter code (Y, C or U; R, A or G; S, G or C; N, A, C, G, or U). A "−" connects paired positions. Position numbers correspond to those in Figure 1.

that the other cloned ligands are representatives of the pool's low-affinity population.

For high-affinity binding, usually a core sequence that includes the aptamer's consensus elements, but not the entire oligonucleotide, is required.[15] The boundaries of the core sequence can be determined from binding experiments with partially hydrolyzed, end-labeled aptamer.[16] Autoradiograms from aptamer **5** boundary experiments (Figure 3) show (1) that, as expected, the consensus motifs are included within the core sequence; (2) that the length of the core sequence is variable, increasing with increasingly stringent binding conditions; (3) that recovery of the boundary species is less efficient than that of longer molecules; and (4) that recovery is incrementally improved as nucleotides are added. These data suggest that while the consensus elements are essential for specific binding, additional binding energy is required for an affinity equivalent to that of the full-length aptamer. This additional binding energy, derived from the added nucleotides, is likely to be sequence-independent. Similar results were obtained with aptamers **1**, **6**, and **9**, the boundaries of which are indicated in the legend of Figure 1.

To confirm the boundary results, affinities of aptamer **5** truncates (transcribed from truncated synthetic templates) were determined directly. As expected, the affinities of the 3′-boundary species, aptamer **11** (Table 1), and of the 5′-boundary species (data not shown) were reduced 4- and 2-fold, respectively, compared to full-length aptamer **5**. The affinity of the composite boundary species, aptamer **12**, which is truncated at both boundaries, was further reduced to 7.3 nM. As expected, the composite boundary species' affinity is substantially improved by the addition of as few as six nucleotides to its 3′ end (aptamers **13**−**15**, Table 1).

To evaluate the specificity of aptamer binding, the affinities of aptamers **5** and **15** and random RNA were determined for proteins unrelated to hnps-PLA_2 (Table 2), including human bFGF and human neutrophil elastase which, like hnps-PLA_2, are small, highly cationic proteins. Aptamer affinities for hnps-PLA_2 are 20−90-fold better than that of random RNA and 25−8000-fold better than for unrelated proteins, and their affinity for unrelated proteins resembles that of random RNA. Thus, binding of evolved aptamers to hnps-PLA_2 is not a nonspecific polyanion/polycation interaction but is sequence-dependent and highly selective.

The melting temperature (T_m) of aptamers **1** and **10** was determined to evaluate the stability of aptamer secondary structure. Moderately higher T_m's were observed in the presence of Ca^{2+} ions than in their absence (Table 3). Increased thermal stability, aptamer **10** (T_m = 28.5 °C) compared with aptamer **1** (T_m = 36.5 °C), is correlated with extension of the upper stem and incorporation of a stable GAAA tetraloop (Figure 1). Nevertheless, under SELEX and binding experiment conditions (TBS, 5 mM Ca^{2+}, 37 °C), a majority of unbound molecules may be unstructured. If stable secondary structure were a prerequisite for binding, affinity might be improved at lower temperatures, where the stability of secondary structure is increased. However, the affinity of aptamer **10** was unchanged at 22 °C compared to at 37 °C (K_d: 0.7 nM), and at 4 °C it actually decreased 10-fold (K_d: 7 nM; Table 2).

We also examined the pH dependence of binding since the 2′-NH_2 moiety of the purine nucleotides is an ionizable group with an estimated pK_a of approximately 6.5. At pH's significantly greater than the pK_a, the SELEX pH (pH 7.4), or higher (pH 8.0 and 8.5), affinities of aptamer **1** are essentially constant (1.8, 1 and 2.6 nM, respectively; Table 3). At pH's near or less than the pK_a (pH 6.8 and 5.8), where ionization of the 2′-NH_2 is expected, affinities are reduced to 11 and 30 nM, respectively. Ionization may cause perturbations of aptamer structure or otherwise alter aptamer/protein interactions in ways that reduce binding affinity.[17]

In addition, aptamer affinity is Ca^{2+}-dependent, as expected given the elution protocol. In the absence of added Ca^{2+} the affinity of aptamer **5** was reduced approximately 10-fold, from 250 pM to 2.5 nM (Table 3).

Aptamer-mediated inhibition of hnps-PLA_2 function was assessed in two activity assays. Initially, activity was evaluated in an in vitro enzymatic assay that was suitable for high-throughput screening. Aptamers showing activity in the screen were then tested in an ex vivo pleural strip contraction assay which utilizes endogenous substrate. Although the tissue assay is more relevant to antagonist activity under physiological conditions, it is unsuitable for initial screenings due to its resource requirements. Aptamers that inhibited enzymatic activity, but not hnps-PLA_2-dependent pleural strip contractions, are considered to be "false positives" and were not further pursued.

The initial screen for functional antagonists was the chromogenic hnps-PLA_2 enzymatic activity assay, described by Reynolds et al.[18] The Reynolds assay is less sensitive and produces fewer "false positives" than enzymatic activity assays using *Escherichia coli* membranes as substrate.[19] The control antagonist, (*R*)-(2-dodecanoylamino)(1-hydroxyhexyl)phosphoglycol,[20] inhibited in a dose-dependent manner with an IC_{50} of 3 μM and a calculated K_i of 1 μM. Aptamer **5** also inhibited in a dose-dependent fashion but with an IC_{50}

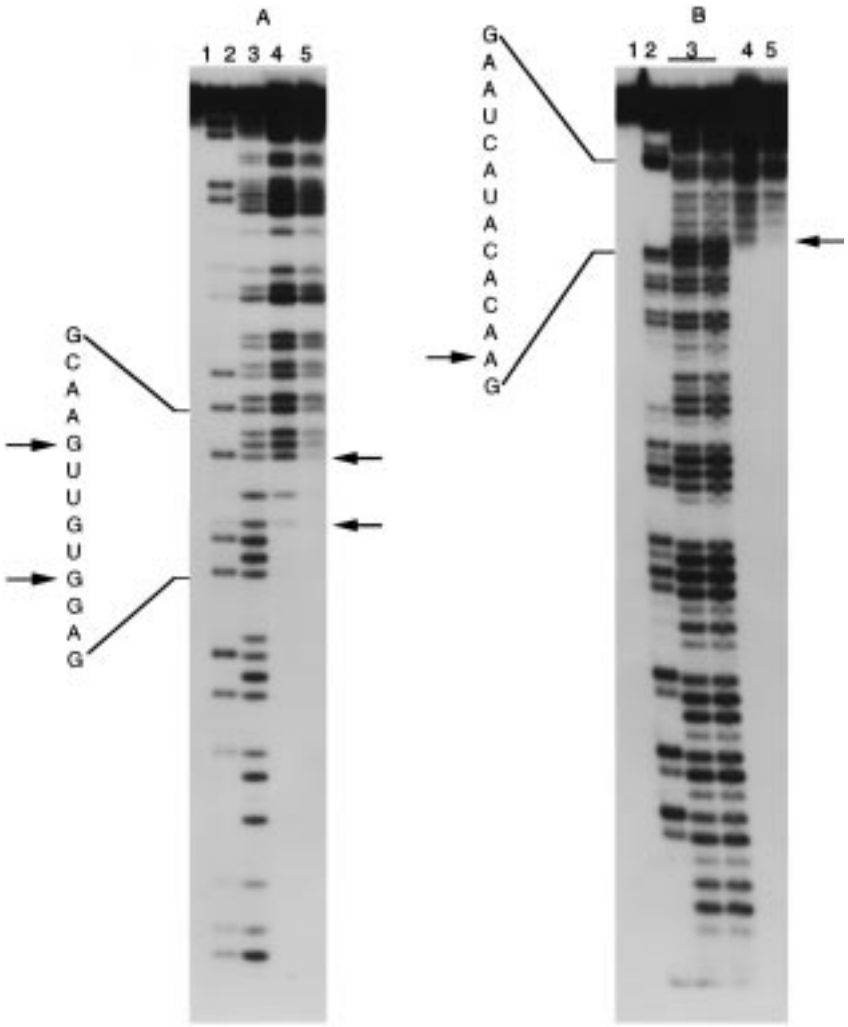

Figure 3. Minimal sequence required for high-affinity binding of aptamer **5**. Binding reactions of ^{32}P-end-labeled, partial alkaline hydrolysates of aptamer **5** and hnps-PLA$_2$ were partitioned by nitrocellulose filtration. The bound RNA was extracted and analyzed on denaturing 8% polyacrylamide gels. Insets show the sequences of the two boundary regions. The insensitivity of pyrimidines to alkaline hydrolysis results in discontinuous hydrolysis ladders (lanes 3−5). Panel A, the 3′ boundary determined with 5′-end-labeled aptamer **5**, bound to 1 nM (lane 4A, low stringency) or 0.2 nM hnps-PLA$_2$ (lane 5A, high stringency): upper arrow, high-stringency 3′ boundary; lower arrow, low-stringency 3′ boundary. Panel B, the 5′ boundary determined with 3′-end-labeled aptamer **5**, bound to 1 nM (lane 4B, low stringency) or 0.2 nM hnps-PLA$_2$ (lane 5B, high stringency): arrow, 5′ boundary. Controls (panels A and B): untreated aptamer **5** (lane 1); RNase T1 partial digestion (lane 2); unselected partial alkaline hydrolysate (lane 3). The variability of band intensities in control lanes 3A,B indicates that purines at all positions are not equally sensitive to alkaline hydrolysis and similarly, in lanes 2A,B, that all Gs are not equally sensitive to RNase T1. Normalization of the intensity of a band of selected material (lanes 4 and 5) to its unselected control (lane 3) indicates the efficiency of recovery of that selected hydrolysis product. Normalized band intensities within a selection lane (ie., within lane 4) are an index of the relative efficiency of recovery of the individual hydrolysis products within that lane. Note that boundary species are recovered less efficiently than longer products.

of 4 nM, a calculated K_i of 0.14 nM, and 93% maximal inhibition (Figure 4A). Similar results were obtained with compounds **1**, **4**, **8**, **10**, **14**, and **15** (Figures 1 and 4B), while aptamer **12** was less active, perhaps due to its lower affinity and/or shorter 3′ sequence. In contrast, at concentrations as high as 300 nM, only partial inhibition (50−60%) was observed for random RNA (Figure 4A). Inhibition by random sequences may be a polyanionic effect similar to that which has been reported for heparin in some assays.[21] However, evolved aptamers inhibit hnps-PLA$_2$ in a sequence-dependent manner.

Truncate **15**, chosen as a family 1 representative, was tested in the tissue-based contraction assay in which guinea pig lung pleural strips serve as a physiological substrate.[22] In this assay, the catalytic activity of

Table 1. Affinity of Aptamer **5** and Its Truncates

aptamers	nt[a]	K_d (nM)	n[b]	sequences[c]
5	98	0.5 ± 0.3	12	A-B-C-D1
11	58	1.9 ± 0.4	2	A-B-C-D2
12	45	7.3 ± 2.9	4	A-C-D2
13	64	0.5 ± 0.3	5	A-C-D3
14	58	2.2 ± 1.2	4	A-C-D4
15	51	1.7 ± 0.2	2	A-C-D5

[a] Number of nucleotides. [b] Number of times the K_d was determined. [c] Sequence A, 5′-GGGAAAAG-3′, is required for initiation of the transcription. Sequence B, 5′-CGAAUCAUACACA-3′, is between the initiation module and the core sequence. Sequence C, 5′-AGACGGCCGGCGCCAUAGCCGAGAUCCGAGGUGUUG-3′, is the core sequence. Sequences D1−D5 are different truncations of the 3′ region: D1, 5′-AACGAUGACAACUCGGUGCUC-CGCCAGAGACCAACCGAGAA-3′; D2, 5′-A-3′; D3, 5′-AACGAUAA-GACCAACCGAGAA-3′; D4, 5′-AGACCAACCGAGAA-3′; D5, 5′-CCGAGAA-3′.

Table 2. Specificity of Family 1 Aptamers: Affinity of Random RNA and Aptamers **5** and **15** for Seven Proteins Unrelated to hnsp-PLA_2

		aptamer	
proteins	random RNA	**5**	**15**
hnps-PLA_2	38[a]	0.4	1.7
hNE[b]	70	40	40
hC1q[c]	1000		1000
HEW lysozyme[d]		580	1300
hthrombin[e]	1400	2100	1000
hbFGF[f]	170	210	160
hIgG[g]	>5000	>5000	4300

[a] K_d (nM). [b] Human neutrophil elastase. [c] Human C1q. [d] Hen egg white lysozyme. [e] Human thrombin. [f] Human basic fibroblast growth factor. [g] Human IgG.

Table 3. Family 1 Aptamers: Summary of the Effects of Temperature, pH, and Ca^{2+} on Affinity and Thermal Stability

		aptamers		
conditions		**1**	**5**	**10**
		Affinities[a]		
TBSC	4 °C			7
	22 °C			0.8
	37 °C			0.7
TBSC	pH 5.8	30		
	pH 6.8	11		
	pH 7.4	1.8		
	pH 8.0	1		
	pH 8.5	2.6		
TBSC	37 °C		0.25	
TBS	37 °C		2.5	
		T_m's[b]		
TBSC		36.5		28.3
TBS		28.5		24.5

[a] K_d (nM). [b] Temperature (°C) at which 50% of the molecules are denatured.

exogenous hnps-PLA_2 on membrane phospholipids results in the release of arachidonic acid and the subsequent formation of primarily cyclooxygenase products leading to the measured contractile responses. Exogenous arachidonic acid bypasses the requirement for hnps-PLA_2, mediates contractions, and constitutes a specificity control.

At 0.3 μM, aptamer **15** effectively inhibits (~70−85%) contractions mediated by 0.02, 0.07, and 0.22 μM hnps-PLA_2(Figure 5A). As is to be expected, when the enzyme is in molar excess, 0.7 μM hnps-PLA_2, inhibition is markedly reduced. In contrast, 0.3 μM control oligonucleotide did not significantly alter hnps-PLA_2 contractile responses at any enzyme concentration, demonstrating again that aptamer-mediated inhibition of hnps-PLA_2 (Figure 5A) is sequence-dependent. In this assay, efficacy or apparent dissociation constant, K_B, of aptamer **15** is 118 ± 26 nM, while that of the previously described indole-based inhibitor LY311727 is 270 ± 50 nM.[6] At a 10-fold higher concentration (3 μM), aptamer **15** virtually abolished all hnps-PLA_2-induced contractile responses (Figure 5B), although the nonspecific activity of the control oligonucleotide was nearly equivalent (Figure 5B). To verify that aptamer-mediated contraction inhibition resulted from blocking hnps-PLA_2 activity, 3 μM aptamer **15** was tested for inhibition of contractile responses elicited by exogenous arachidonic acid. Contractile responses were not altered (Figure 6), demonstrating that aptamer **15** inhibition is specific for the hnps-PLA_2 hydrolysis step.

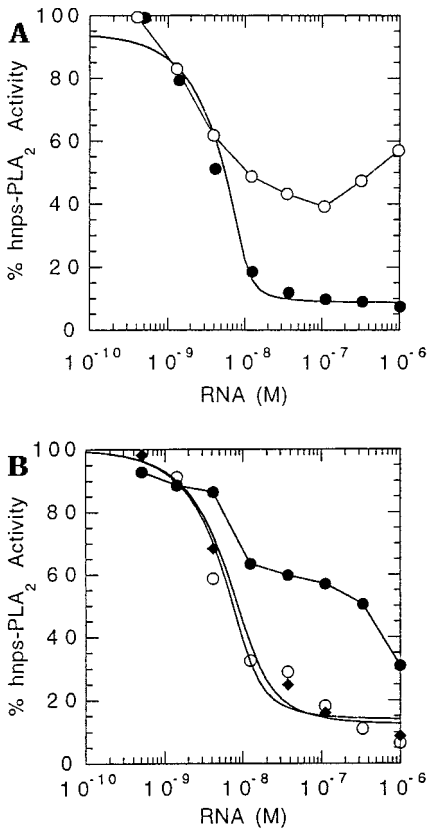

Figure 4. Inhibition of hnps-PLA_2 enzymatic activity mediated by aptamers **5**, **12**, **14**, and **15**. The standard chromogenic assay of hnps-PLA_2 enzymatic activity was performed in the presence of increasing concentrations of aptamer (see methods). Results are normalized to enzymatic activity in the absence of any competitor. Each set of experiments was monitored with the control inhibitor (*R*)-(2-dodecanoylamino)-(1-hexyl)phosphoglycol. Panel A: aptamer **5** (●) or random 2′-NH_2-pyrimidine RNA (○). Panel B: aptamer **12** (●), **14** (◆), or **15** (○).

Conclusion

A family of sequence-related aptamers, isolated by SELEX methodology from a sequence-randomized pool of 3×10^{14} 2′-NH_2-pyrimidine, 2′-OH-purine RNA molecules, bound hnps-PLA_2 specifically and with high affinity (120−850 pM). In a standard hnps-PLA_2 activity assay, the aptamers inhibited enzymatic activity at mole fractions of substrate concentration of $<4 \times 10^{-6}$, with IC_{50}'s ranging from 0.2 to 4 nM which constitute up to a 5000-fold improvement over the control inhibitor (*R*)-(2-dodecanoylamino)(1-hydroxyhexyl)phosphoglycol.

The complexities of hnps-PLA_2 functional assays are such that, in and of itself, inhibition of enzymatic activity is not a demonstration of direct interaction between inhibitor and enzyme.[23] Functional activity of in vitro assays can be prevented by binding the enzyme's active site, by binding an accessory site on the enzyme, or binding to aggregated substrate. The enzyme's preference for aggregates over single molecules in solution may be due to a greater resemblance of aggregates to cell membranes, the enzyme's natural in vivo substrate, and has raised questions concerning appropriate artificial substrates.[24] Each of the three types of binding interactions yields inhibitors with IC_{50}'s in the micromolar range (100 nM to 10 μM).[25] In the

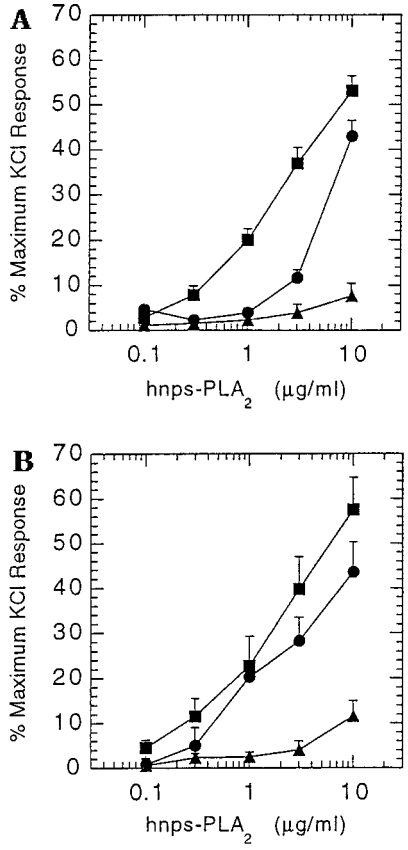

Figure 5. Aptamer **15**-mediated inhibition of hnps-PLA$_2$-induced contractions of guinea pig lung pleural strips. Contractions mediated by increasing concentrations of hnps-PLA$_2$ were assayed in the presence of saline or aptamer. The results are the means and standard errors of N independent determinations. Panel A: saline (■), $N = 8$; 0.3 μM aptamer **15** (●), $N = 4$; 3 μM aptamer **15** (▲), $N = 4$. Apparent $K_B = 118 \pm 26$ nM. Panel B: saline (■), $N = 8$; 0.3 μM random RNA (●), $N = 4$; 3 μM random RNA (▲), $N = 4$. Apparent $K_B = 190 \pm 54$ nM.

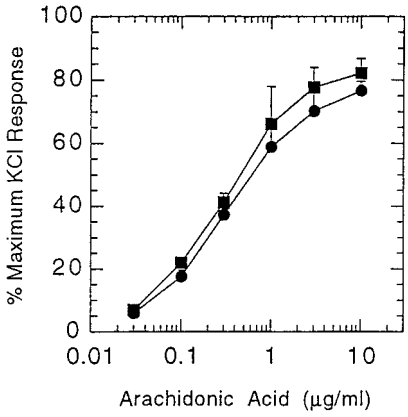

Figure 6. Arachidonic acid-mediated contractions of guinea pig lung pleural strips in the presence of aptamer **15**. Contractions mediated by increasing concentrations of arachidonic acid were assayed in the presence of saline (■), $N = 4$, or 3 μM aptamer **15** (●), $N = 4$. The results are the means and standard errors of N independent determinations. Apparent $K_B = 28 \pm 31$ mM.

Reynolds chromogenic assay which gives fewer "false positives" than do *E. coli* membrane-based assays,[19] the IC$_{50}$'s of aptamers range from 0.4 to 4 nM, as noted above, and are superior to known active site inhibitors (see below).

Although we have not determined the mechanism, our data suggest that inhibition is dependent on aptamer binding to a site on hnps-PLA$_2$. In the chromogenic assay, the low aptamer/substrate molar ratios and the nearly complete, apparently competitive inhibition support aptamer/hnps-PLA$_2$ interaction. Noncompetitive or uncompetitive inhibition is more likely for an aptamer/substrate-based mechanism. Aptamer/enzyme interaction is also supported by the high affinity of the binding interaction, by the correlation of affinity and inhibition and their similar sequence dependence, and by the apparent 1:1 stoichiometry of aptamer to hnps-PLA$_2$ for inhibition.

More importantly, in tissue-based assays using endogenous substrate, aptamer **15** inhibits exogenous hnps-PLA$_2$-mediated contractions of guinea pig pleural strips with a K_B of 118 ± 26 nM. As expected, aptamer **15** did not inhibit contractions mediated by exogenous arachidonic acid, demonstrating that aptamer-based inhibition is neither a cellular toxicity effect nor inhibition of a reaction downstream to hnps-PLA$_2$ and thus, in the biological sense of the word, is apparently specific for the hnps-PLA$_2$ hydrolysis step. As in the in vitro assay, inhibition of contractions appears to be dependent on a 1:1 stoichiometry of aptamer to hnps-PLA$_2$, since inhibition diminishes in molar excess enzyme. Thus, the aptamers appear to interact with the enzyme in such a way as to block substrate access to the active site. The interesting questions of defining the binding site and determining if any part of the aptamer fits into the active site require additional study. However, both binding the active site and blocking substrate access through binding the enzyme provide suitable mechanisms of inhibition for an in vivo antagonist.

Phosphorothioate-modified deoxy oligonucleotide antagonists of hnps-PLA$_2$ that contain a G-C-rich sequence and two potential G-quartet motifs have been described.[26] These oligonucleotides, developed as antisense antagonists, apparently act as antagonists of enzyme function. More recently, a low-affinity and weakly inhibitory family of modified deoxy pentanucleotides has been developed by SURF (*s*ynthetic *u*nrandomization of *r*andomized *f*ragments) technology.[27] That neither the phosphorothioate nor the SURF oligomers share sequence or structural motifs with our aptamers is not surprising. Aptamer structure is determined in part by backbone chemistry and in part by nucleoside modifications.[28] In addition, SELEX technology itself often provides more than one solution for a given target.[29]

In our initial SELEX against hnps-PLA$_2$, partitioned by nitrocellulose filtration alone, aptamers that inhibited function were rare.[8] Thus, the success of the present SELEX appears to support our partition and elution strategy: bead-mediated target immobilization and directed/competitive elution of aptamers bound near the active site. To our knowledge, this was the first SELEX application of immobilization and directed/competitive elution to a protein target. We have now used refinements of this strategy to isolate antagonists of wheat germ agglutinin,[9] human L-selectin,[10,11] and both human and murine P-selectin.[12]

The chromogenic enzymatic and pleural strip contraction assays provide a direct comparison of the activities

of aptamer **15** and LY311727, a low-molecular-weight indole-based antagonist. Even though the molecules are very different, both antagonists are specific for hnps-PLA_2 and lack cellular toxicity. However, aptamer **15** (IC_{50}: 4 nM at a mole fraction of 4×10^{-6}; K_B: 118 ± 26 nM) is a more active inhibitor than LY311727 (IC_{50}: 13 mM at a mole fraction of 14×10^{-3}; K_B: 270 ± 50 nM). Furthermore, the activity of aptamer **15** is equivalent to that of a recently described, indole-3-glyoxamide antagonist, LY315920 (IC_{50}: 9 nM at a mole fraction of 7×10^{-6}; K_B: 83 nM).[30]

Like the aptamers and indole-based molecules themselves, the processes that produced them are radically different. SELEX technology, which is extremely rapid and requires no knowledge of target structure, yields high-affinity ligands to the target by cycles of selection and amplification. Diversity resides primarily in vast numbers of sequences and the resulting structures.[31] Diversity can be further increased by the use of modified libraries.[32] For example, the 2′-aminopyrimidine nucleotides that were used in the hnps-PLA_2 SELEX increase nuclease resistance of oligonucleotides.[33] On the other hand, rational drug design requires detailed structural information, has diverse chemistries, and proceeds by deliberate, sequential modifications of a lead compound.[34] The present work demonstrates that the two processes can develop antagonists with very similar activities. By virtue of its in vitro activity, aptamer **15**, like LY311727, is a likely candidate for in vivo evaluation.

Experimental Section

Abbreviations. hnps-PLA_2, human nonpancreatic secretory phospholipase A_2, Ab-gel, antibodies against hnps-PLA_2 covalently coupled to agarose beads; TBS, Tris-buffered saline (25 mM Tris, pH 7.4, 150 mM NaCl); TBSC, TBS + 5 mM $CaCl_2$; TKC, Tris potassium calcium buffer (25 mM Tris, 2.5 mM $CaCl_2$, 100 mM KCl); HSA, human serum albumin; SELEX, *s*ystematic *e*volution of *l*igand by *ex*ponential enrichment; nt, nucleotide; ds, double stranded; ss, single stranded; K_d, equilibrium dissociation constant.

Chemical Methods. Materials. The hnps-PLA_2, rabbit anti-hnps-PLA_2 polyclonal antibody, and 1,2-bis(heptanoylthio)-1,2-dideoxy-*sn*-glycero-3-phosphorylcholine (di-C7-thio-PC) used in these experiments were supplied by Eli Lilly & Co. Hen egg white lysozyme (6× crystallized) was provided by Dr. S. C. Gill. Human neutrophil elastase, human thrombin, human C1q, and human basic fibroblast growth factor were provided by Dr. S. Jayasena, Dr. D. Tasset, Dr. G. Bieseker, and Dr. N. Janjic, respectively. Human IgG was purchased from Sigma (Saint Louis, MO). The 2′-NH_2-modified CTP and UTP were produced as previously described.[35] Single-stranded deoxy oligonucleotide templates and primers were synthesized by Operon Technologies, Inc., Alameda, CA: SELEX template sequence, 5′-GGGAAAAGCGAATCATACACAAG-50N-GCTCCGCCAGAGACCAACCGAGAA-3′; 5′-primer sequence, 5′-TAATACGACTCACTATAGGGAAAAGCGAATCATACACAAGA-3′; 3′-primer sequence, 5′-TTCTCGGTTGGTCTCTGGCTTATC-3′. HSA and 5,5′-dithiobis(2-nitrobenzoic acid) (DTNB) were purchased from Sigma, and Triton X100 was from Fluka (Ronkonkoma, NY). All other reagents and chemicals were purchased from commercial sources.

SELEX. Both nitrocellulose partitioning (rounds 6, 7, 10, and 11) and hnps-PLA_2 immobilized on beads via an anti-hnps-PLA_2 polyclonal antibody (rounds 1−5, 8, and 9) were used to separate free from bound RNA.

Polyclonal anti-hnps-PLA_2 agarose beads were prepared from an ammonium sulfate-precipitated, anion-exchange-purified immunoglobulin fraction of an hnps-PLA_2-immunized rabbit. Oxidized immunoglobulins were bound to hydrazine-activated agarose beads (CarboLink coupling gel, Pierce, Rockford, IL) according to the manufacturer's instructions. The resulting immunoglobulin density was estimated to be 1.2 mg/mL of gel. Coupling of hnps-PLA_2 was accomplished by incubating 50 μL of Ab-gel with 500 μL of 2 μM hnps-PLA_2 in TBSC for 2 h at 37 °C. The washed gel, which was resuspended in 500 μL of TBSC and stored at 4 °C, had a calculated hnps-PLA_2 density of 0.2 pmol/μL of gel, assuming that 1% of the Ig fraction is anti-hnps-PLA_2 Ab and a stochiometry of 1 molecule of hnps-PLA_2 bound/antibody molecule.

For rounds in which immobilized hnps-PLA_2 was used to partition unbound RNA from hnps-PLA_2/RNA complexes, RNA was incubated with washed hnps-PLA_2-gel in a siliconized column for 5 min at 37 °C with constant agitation. Unbound RNA was removed by extensive washing with TBSC. Bound RNA was eluted as two fractions; the first fraction was eluted with calcium-free buffer, TBS; the second fraction was eluted with free polyclonal anti-hnps-PLA_2 Ab in calcium-free buffer, Ab/TBS. Each fraction was processed separately. The results reported here are for Ab/TBS-eluted RNA.

For rounds in which partitioning was accomplished by nitrocellulose filter binding, free hnps-PLA_2 and RNA were incubated for 5 min at 37 °C, filtered through TBSC prewashed nitrocellulose filters, and then washed with 3 mL of TBSC. RNA/hnps-PLA_2 complexes, bound to nitrocellulose membranes or eluted from immobilized hnps-PLA_2, were heated at 90 °C for 5 min in 1% SDS, 2% β-mercaptoethanol. RNA was isolated by phenol/chloroform extraction and alcohol precipitation as previously described.[36]

Extracted RNAs were reverse-transcribed and amplified by PCR using the primers described in the SELEX methodology section. Double-stranded DNA was transcribed with T7 polymerase using 1 mM 2′-hydroxy ATP and GTP and 1 mM 2′-amino UTP and CTP at 37 °C for 3 h. The full-length RNA was purified on a 12% denaturing gel. The material was extracted from the gel by a crush and soak procedure and ethanol-precipitated using NaOAc salt. After resuspension in water, the concentration of RNA was estimated from its absorption at 260 nm, using an extinction coefficient of 40 μg of oligonucleotide/mL/optical density unit.

Nitrocellulose Filter Partitioning. Since most proteins and protein/RNA complexes bind nitrocellulose, nitrocellulose filtration was used to determine the affinity of aptamers for hnps-PLA_2 and other proteins, as previously described.[36] Filter disks (nitrocellulose/cellulose acetate mixed matrix, 0.45-μm pore size; Millipore) were placed on a vacuum manifold and washed with 5 mL of TBSC buffer under vacuum. Reaction mixtures, containing ^{32}P-labeled RNA pools and hnps-PLA_2, were incubated in TBSC for 5 min at 37 °C, filtered, and then immediately washed with 5 mL of TBSC. The filters were air-dried and counted in a Beckman LS 2000 liquid scintillation counter without fluorophore.

The equilibrium dissociation constant, K_d, for an RNA pool or specific ligand that binds monophasically is given by the equation:

$$K_d = [P_f][R_f]/[RP]$$

where $[R_f]$ is free RNA concentration, $[P_f]$ is free protein concentration, and K_d is equilibrium dissociation constant. A rearrangement of this equation, in which the fraction of RNA bound at equilibrium is expressed as a function of the total concentration of the reactants, was used to calculate the K_d's of monophasic binding curves:[37]

$$q = [P_T] + [R_T] + K_d - ([P_T] + [R_T] + K_d)^2 - 4[P_T][R_T]^{1/2}$$

where q is fraction of RNA bound, $[P_T]$ is total protein concentration, and $[R_T]$ is total RNA concentration. K_d's were determined by least-squares fits, using the graphics program Kaleidagraph (Synergy Software, Reading, PA).

Cloning and Sequencing. PCR of the cDNA of eleventh round Ab/TBS-eluted RNA was performed with primers which

contain a recognition site for the restriction endonucleases *Hin*dIII and *Bam*HI. Using these restriction sites the DNA sequences were inserted directionally into the pUC18 vector. These recombinant plasmids were transformed into *E. coli* strain XL-1 blue (Stratagene, La Jolla, CA). Plasmid DNA was prepared according to the alkaline hydrolysis method.[38] Approximately 40 clones were sequenced with the Sequenase sequencing kit (United States Biochemical Corp., Cleveland, OH).

Aptamer Truncation. Minimal aptamer sequences necessary for high affinity binding to sPLA$_2$ were determined by "boundary experiments", as previously described.[16] For 3′-boundary determination, aptamers were 5′-end-labeled with [γ-^{32}P]ATP using T4 polynucleotide kinase. 5′-Boundaries were established with 3′-end-labeled ligands using [γ-^{32}P]pCp and T4 RNA ligase. After partial alkaline hydrolysis, radiolabeled aptamers were incubated with hnps-PLA$_2$ at concentrations ranging from 0.4 to 28 nM, and hnps-PLA$_2$/RNA complexes were separated from unbound RNA by nitrocellulose partitioning. RNA/hnps-PLA$_2$ complexes were extracted from the filters, and the RNA was electrophoresed on high-resolution denaturing polyacrylamide gels. The discontinuous banding patterns observed on gels are due to the resistance of phosphodiester bonds of 2′-NH$_2$-pyrimidines to alkaline hydrolysis. Only molecules that include both the ^{32}P end labeled and the intact binding site are visualized on autoradiograms of gels. Molecules which contain the binding site but no end label are undetectable. Molecules that contain only a portion of the binding site fail to bind hnps-PLA$_2$ and are lost during filtration. The fastest migrating band corresponds to the boundary species. Two electrophoretic markers were included to aid in identifying boundary positions: (1) the partial alkaline hydrolysate without exposure to protein and (2) a partial RNase T1 digest of the same labeled ligand. RNase T1 specifically hydrolyzes the phosphodiester bond 3′ to guanine ribonucleotides.

Melting Temperature (T_m) Measurements. Melting profiles were determined on a Cary model 1E spectrophotometer. Oligonucleotides (130−160 nM) were heated to 95 °C in TBS, pH 7, and cooled to room temperature prior to the melting profile determination. Melting profiles were generated by recording the absorbance at 260 nm while the sample was heated at the rate of 1 °C/min from 1 to 80 °C. Calcium chloride was added to the samples (5 mM final concentration) and the procedure repeated. Alpha curves were constructed, and the T_m was calculated as previously described.[39]

Aptamer 15. Oligonucleotides used in the pleural strip assays were from a scaled-up (40 mL) standard transcription. Double-stranded template was generated by annealing appropriate complementary synthetic ssDNAs (Operon Technologies, Inc.). The sequences of synthetic ssDNAs were derived from aptamer **5 (**Table 1**)**. In turn, the sequence of aptamer **15** is determined by the synthetic template. The transcribed aptamer was purified by gel electrophoresis. Analysis by capillary gel electrophoresis indicated that 57.5% of the molecules were 51 nts in length, 33.5% were 1−2 nts longer, 7.6% were 1−4 nts shorter, and <1.5% were >4 nts shorter.

Activity Assay Methodology. Inhibition of hnps-PLA$_2$ Enzymatic Activity. Activity assays were carried out following the general procedures outlined by Reynolds et al.[18] and used the following solutions: (1) DTNB solution (5 mM) was prepared weekly by dissolving 20 mg of DTNB in 10 mL of H$_2$O and titrating to pH 7 with 0.1 N NaOH; (2) 10×TKC containing 250 mM Tris, pH 7.5 or 8.0 as indicated, 1000 mM KCl, 25−100 mM CaCl$_2$, and 1% HSA; (3) hnps-PLA$_2$ assay solution, 220 in 1XTKC; (4) substrate solution containing 1 mM di-C7-thio-PC), 0.28 mM Triton X100, 0.12 mM DTNB, and the corresponding 1×TKC solution; (5) inhibitor solutions for a given inhibitor consisted of eight different concentrations obtained by 3× serial dilutions in 1×TKC.

Assays were carried out in 96-well microplates. To each well was added 200 μL of substrate solution followed by 10 μL of appropriate inhibitor solution or blank in 1×TKC buffer and mixed. To start the reaction 10 μL of hnps-PLA$_2$ assay solution was added and mixed (final hnps-PLA$_2$ concentration, 10 nM). Negative controls were identical except for the omission of hnps-PLA$_2$. Samples were read at 405 nm in a Bio-Tek EL312e microplate reader at 5, 10, 15, 20, 25, and 30 min after addition of hnps-PLA$_2$ at 40 °C. Reaction rates were determined by plotting the OD vs time and determining the slope. These reaction rates were used to determine the percent activity, where 100% activity is defined as the rate for hnps-PLA$_2$ without inhibitor and 0% activity as the rate in absence of hnps-PLA$_2$ and inhibitor. Inhibition plots were created by percent activity vs concentration of inhibitor.

To determine K_i values, we have assumed competitive inhibition and 1:1 stoichiometries for hnps-PLA$_2$:substrate and hnps-PLA$_2$:RNA. We have used a K_m for the substrate interaction with hnps-PLA$_2$ of 0.5 mM.[18] We have independently measured this K_m at values that range from 0.4 to 0.65 mM. Inhibition data were fit to a standard competition binding polynomial allowing the K_i to vary, and where possible, the maximum and minimum percent activities were allowed to vary.[37]

Tissue Assay. General: The preparation of the guinea pig lung pleural strip has been described previously.[22] Briefly, male Hartley strain guinea pigs (500−700 g) were killed by cervical dislocation and their heart and lungs removed intact and placed in aerated (95% O$_2$:5% CO$_2$) Krebs solution of the following composition (mM): NaCl, 118.2; KCl, 4.6; CaCl$_2$·2H$_2$O, 2.5; MgSO$_4$·7H$_2$O, 1.2; NaHCO$_3$, 24.8; KH$_2$PO$_4$, 1.0; and dextrose, 10.0. Dorsal pleural strips (4 × 1 × 25 mm) were dissected from intact parenchymal segments (8 × 4 × 25 mm) cut parallel to the outer edge of the lower lung lobes. Two adjacent pleural strips, obtained from a single lobe and representing a single tissue sample, were tied at either end and independently attached to a metal support rod. One rod was attached to a Grass force-displacement transducer (FTO3C). Changes in isometric tension were displayed on a Modular Instruments monitor and thermal recorder. All tissues were placed in 10-mL jacketed tissue baths with continuous aeration and maintained at 37 °C. Pleural strips from the opposite lobes of the lung were used for paired experiments. Preliminary data generated from tension−response curves demonstrated that resting tension of 800 mg was optimal. The tissues were allowed to equilibrate for 45 min as the bath fluid was changed periodically.

Cumulative Concentration−Response Curves: Initially tissues were primed by challenging them three times with KCl (40 mM) to test tissue viability and to obtain a consistent response. After recording the maximal response to KCl, the tissues were washed and allowed to return to baseline before the next challenge. Cumulative concentration−response curves were obtained from pleural strips by increasing the agonist concentration in the tissue bath by half-log increments while the previous concentration remained in contact with the tissues.[40] Agonist concentration was increased after reaching the plateau of the contraction elicited by the preceding concentration. One concentration−response curve was obtained from each tissue. To minimize variability between tissues obtained from different animals, contractile responses were expressed as a percentage of the maximal response obtained with the final KCl challenge. When studying the effects of various drugs on the contractile effects of the agonists, the drugs and their respective vehicles were added to the tissues 30 min prior to starting the concentration−response curves.

Statistical Analysis: Data from different experiments were pooled and are presented as a percentage of the maximal KCl responses (mean ± SE). Concentration−response curves were analyzed using a three-parameter logistic model.[41] The three modeled parameters included: the maximum tissue response (MAX), the ED$_{50}$, the concentration of agonist required to elicit 50% of the maximal response, and the slope of the curves. Because experiments were performed on tissue pairs (control (vehicle) and treated (drug)), the logistic model was fit simultaneously to the pairs of tissues in order to obtain parameter estimates that were free of animal-to-animal varia-

tion. Thus for each tissue pair, estimates of the ED_{50} ratios (ED_{50} treated/ED_{50} control) and estimates of the MAX ratios (MAX treated/MAX control) were determined. When multiple concentrations of test agent were examined in several experiments, a composite of the control curves was used to estimate an apparent dissociation constant (app K_B). Drugs and chemicals: arachidonic acid (Nu Chek Prep, Inc., Elysian, MN), oligonucleotide inhibitors (NeXstar Pharmaceuticals Inc., Boulder, CO). Cloned hnps-PLA_2 was expressed and purified from Syrian hamster AV12 cells.

Acknowledgment. The authors thank Bruce Feistner, Heather Shannon, and Dr. Dan Drolet for technical assistance and Dr. Barry Polisky for helpful discussions regarding the SELEX experiments and manuscript as well as Dr. Steve Ringquist for his serious critique of the manuscript.

References

(1) Kramer, R. M.; Hession, C.; Johansen, B.; Hayes, G.; McGray, P.; Chow, E. P.; Tizard, R.; Pepinsky, R. B. Structure and Properties of a Human Nonpancreatic Phospholipase A_2. *J. Biol. Chem*. **1989**, *264*, 5768−5775.

(2) Rintala, E. M.; Nevalainen, T. J. Group II Phospholipase A_2 in Sera of Febrile Patients with Microbiologically or Clinically Documented Infections. *Clin. Infect. Diseases* **1993**, *17*, 864−870.

(3) Dennis, E. A. Diversity of Group Types, Regulation, and Function of Phospholipase A_2. *J. Biol. Chem*. **1994**, *269*, 13057−13060.

(4) Hack, C. E.; Wolbink, G.; Schalkwijk, C.; Speijer, H.; Hermens, W.; van den Bosh, H. A Role for Secretory Phospholipase A_2 and C-Reactive Protein in the Removal of Injured Cells. *Immunol. Today* **1997**, *18*, 111−115.

(5) Chilton, F. Would the Real Role(s) for Secretory PLA_2 Please Stand Up. *J. Clin. Invest*. **1996**, *97*, 2161−2162.

(6) Schevitz, R. W.; Bach, N. J.; Carlson, D. G.; Chirgadze, N. Y.; Clawson, D. K.; Dillard, R. D.; Draheim, S. E.; Hartley, L. W.; Jones, N. D.; Mihelich, E. D.; Olkowski, J. L.; Snyder, D. W.; Sommers, C.; Wery, J.-P. Structure-Based Design of the First Potent and Selective Inhibitor of Human non-Pancreatic Secretory Phospholipase A_2. *Nature Struct. Biol*. **1995**, *2*, 458−465.

(7) Tuerk, C.; Gold, L. Systematic Evolution of Ligands by Exponential Enrichment: RNA Ligands to Bacteriophage T4 DNA Polymerase. *Science* **1990**, *249*, 505−510.

(8) Chang, Y.; Parma, D. Unpublished results.

(9) Bridonneau, P.; Parma, D. Unpublished results.

(10) O'Connell, D.; Koenig, A.; Jennings, S.; Hicke, B.; Han, H.; Fitzwater, T.; Chang, Y.; Varki, N.; Parma, D.; Varki, A. Calcium-Dependent Oligonucleotide Antagonists Specific for L-Selectin. *Proc. Natl. Acad. Sci. U.S.A*. **1996**, *93*, 5883−5887.

(11) Hicke, B. J.; Watson, S. R.; Koenig, A.; Lynott, K.; Bargatze, R. F.; Chang, Y.; Ringquist, S.; Moon Mc-Dermott, L.; Jennings, S.; Fitzwater, T.; Han, H.; Varki, N.; Albinana, I.; Willis, M.; Varki, A.; Parma, D. DNA Aptamers Block L-Selectin Function in vivo. *J. Clin. Invest*. **1996**, *98*, 2688−2692.

(12) Jenison, R.; Parma, D. Unpublished results.

(13) Cornish-Bowden, A. Nomenclature for Incompletely Specified Base in Nucleic Acid Sequences: Recommendation 1984. *Nucleic Acids Res*. **1985**, *13*, 3021−3030.

(14) Woese, C. R.; Pace, N. R. Probing RNA Structure, Function, and History by Comparative Analysis. In *The RNA World*; Gesteland, R. F., Atkins, J. F., Eds.; Cold Spring Harbour Laboratory Press: Cold Spring Harbour, NY, 1993; pp 91−117.

(15) Jellinek, D.; Green, L.; Bell, C.; Janjic, N. Inhibition of Receptor Binding by High-Affinity RNA Ligands to Vascular Endothelial Growth Factor. *Biochemistry* **1994**, *33*, 10450−10456.

(16) Carey, J.; Cameron, V.; de Haseth, P. L.; Uhlenbeck, O. C. Sequence-specific Interaction of R17 Coat Protein with its Ribonucleic Acid Binding Site. *Biochemistry* **1983**, *22*, 2601−2610.

(17) Saenger, W. RNA Structure. In *Principles of Nucleic Acid Structure*; Cantor, C. R., Ed.; Springer-Verlag: New York, 1984; pp 242−252.

(18) Reynolds, R. J.; Hughes, L. L.; Denis, E. A. Analysis of Human Synovial Fluid Phospholipase A2 on Short Chain Phasphatidylcholine-Mixed Micelles: Development of a Spectrophotometric Assay Suitable for a Microtiterplate Reader. *Anal. Biochem*. **1992**, *204*, 190−197.

(19) Dillard, R. D.; Bach, N. J.; Draheim, S. E.; Berry, D. R.; Carlson, D. G.; Chirgadze, N. Y.; Clawson, D. K.; Hartley, L. W.; Jonhson, L. M.; Jones, N. D.; McKinney, E. R.; Mihelich, E.; Olkowski, J. L.; Schevitz, R. W.; Smith, A. C.; Snyder, D. W.; Sommers, C. D.; Wery, J. Indole Inhibitors of Human Nonpancreatic Secretory Phospholipase A_2. 1. Indole-3-acetamides. *J. Med. Chem*. **1996**, *39*, 5119−5136.

(20) Thunnissen, M. G. M.; Ab, E.; Kalk, K. H.; Drenth, J.; Dijkstra, B. W.; Kuipers, O. P.; Dijkman, R.; de Haas, G. H.; Verheij, H. M. X-ray Structure of Phospholipase A_2 Complexed with a Substrate-derived Inhibitor. *Nature* **1990**, *347*, 689−691.

(21) Parks, T. P.; Lukas, S.; Hoffman, A. F. Purification and Characterization of a Phospholipase A_2 from Human Osteoarthritic Synovial Fluid. In *Phospholipase A_2*; Wong, P. Y. K., Dennis, E. A., Eds.; Plenum Press: New York, 1990; pp 55−79.

(22) Snyder, D. W.; Sommers, C. D.; Bobbitt, J. L.; Mihelich, E. D. Characterization of the Contractile Effects of Human Recombinant non-Pancreatic Secretory Phospholipase A_2 and Other PLA_2s on Guinea Pig Lung Pleural-strips. *J. Pharmacol. Exp. Ther*. **1993**, *266*, 1147−1155.

(23) Yuan, W.; Quin, D. M.; Sigler, P. B.; Gelb, M. H. Kinetic and Inhibition Studies of Phospholipase A_2 with Short-Chain Substrates and Inhibitors. *Biochemistry* **1990**, *29*, 6082−6094.

(24) Reynolds, L.; Mihelich, E. D.; Dennis, E. A. Inhibition of Venom Phospholipase A_2 by Manoalide and Manoalogue. *J. Biol. Chem*. **1991**, *266*, 16512−16517.

(25) Connoly, S.; Robinson, D. H. The Search for Inhibitors of the Phospholipase A_2. *Exp. Opin. Ther. Patents* **1995**, *5*, 673−683.

(26) Bennet, C. F.; Chiang, M.; Wilson-Lingardo, L.; Wyatt, J. R. Sequence Specific Inhibition of Human Type II Phospholipase A_2 Enzyme Activity by Phosphorothioate Oligonucleotides. *Nucleic Acids Res*. **1994**, *22*, 3202−3209.

(27) Davis, P. W.; Vickers, T. A.; Wilson-Lingardo, L.; Wyatt, J. R.; Guinosso, C. J.; Sanghvi, Y. S.; Debaets, E. A.; Acevedo, O. L.; Cook, P. D.; Ecker, D. J. Drugs Leads from Combinatorial Phosphodiester Libraries. *J. Med. Chem*. **1995**, *38*, 4363−4366.

(28) Gold, L.; Polisky, B.; Uhlenbeck, O.; Yarus, M. Diversity of Oligonucleotide Functions. *Annu. Rev. Biochem*. **1995**, *64*, 763−797.

(29) Jellinek, D.; Lynott, C. K.; Rifkin, B. D.; Janjic, N. High-affinity RNA Ligands to Basic Fibroblast Growth Factor Inhibit Receptor Binding. *Proc. Natl. Acad. Sci. U.S.A*. **1993**, *90*, 11227−12231.

(30) Draheim, S. E.; Bach, N. J.; Dillard, R. D.; Berry, D. R.; Carlson, D. G.; Chirgadze, N. Y.; Clawson, D. K.; Hartley, L. W.; Jonhson, L. M.; Jones, N. D.; McKinney, E. R.; Mihelich, E.; Olkowski, J. L.; Schevitz, R. W.; Smith, A. C.; Snyder, D. W.; Sommers, C. D.; Wery, J. Indole Inhibitors of Human Nonpancreatic Secretory Phospholipase A_2. 3. Indole-3-glyoxamides. *J. Med. Chem*. **1996**, *39*, 5159−5175.

(31) Gold, L. Oligonucleotides as Research Diagnostic, and Therapeutic Agents. *J. Biol. Chem*. **1995**, *270*, 13581−13584.

(32) Lin, Y.; Gill, S. C.; Jayasena, S. D. Modified RNA Sequence Pools for *in vitro* Selection. *Nucleic Acids Res*. **1994**, *22*, 5229−5234.

(33) Lee, S.; Sullenger, B. A. Isolation of a Nuclease-Resistant Decoy RNA That Can Protect Human Acetylcholine Receptors from Myasthenic Antibodies. *Nature Biotechnol*. **1996**, *15*, 41−45.

(34) Blundell, T. L. Stucture-Based Drug Design. *Nature* **1996**, *384*, 23−26.

(35) Pieken, W. A.; Olsen, D. B.; Benseler, F.; Aurup, H.; Eckstein, F. Kinetic Characterization of Ribonuclease-Resistant 2′-Modified Hammerhead Ribozymes. *Science* **1991**, *253*, 314−317.

(36) Schneider, D.; Tuerk, C.; Gold, L. Selection of High Affinity RNA Ligands to the Bacteriophage R17 Coat Protein. *J. Mol. Biol*. **1992**, *228*, 862−869.

(37) Gill, S. C.; Weitzel, S. E.; von Hippel, P. H. Escherichia Coli Sigma70 and NusA Proteins I. Binding Interactions with Core RNA Polymerase in Solution and Within the Transcription Complex. *J. Mol. Biol*. **1991**, *220*, 307−324.

(38) Zhou, C.; Yang, Y.; Jong, A. Y. Mini-Prep in Ten Minutes. *Biotechniques* **1990,** *8*, 172−173.

(39) Marky, L. A.; Breslauer, K. J. Calculating Thermodynamic Data for Transitions of Any Molecularity from Equilibrium Melting Curves. *Biopolymers* **1987**, *26*, 1601−1620.

(40) van Rossum, J. M. Cumulative Dose−Response Curves. II. Technique for the Making of Dose−Response Curves in Isolated Organs and the Evaluation of Drug Parameters. *Arch. Int. Pharmacodyn. Ther*. **1963**, *143*, 299−330.

(41) De Lean, A.; Munson, P. J.; Rodbard, D. Simultaneous Analysis of Families of Sigmoidal Curves: Application to Bioassay, Radioligand Assay and Physiological Dose−Response Curves. *Am. J. Physiol*. **1978**, *235*, E97−E102.

JM970579K